Supramolecular Chemistry
Publication details, including instructions for authors and subscription information:
http://www.informaworld.com/smpp/title~content=t713649759

Cucurbit[*n*]urils (*n*=7, 8) binding of camptothecin and the effects on solubility and reactivity of the anticancer drug

Nan Dong[ab]; Sai-Feng Xue[b]; Qian-Jiang Zhu[b]; Zhu Tao[bc]; Yu Zhao[a]; Lei-Xiang Yang[a]
[a] Institute of Materia Medical, College of Pharmaceutical Science, Zhejiang University, Hangzhou, P R China [b] Key Laboratory of Macrocyclic and Supramolecular Chemistry of Guizhou Province, Guizhou University, Guiyang, P R China [c] Institute of Applied Chemistry, Guizhou University, Guiyang, P R China

To cite this Article Dong, Nan , Xue, Sai-Feng , Zhu, Qian-Jiang , Tao, Zhu , Zhao, Yu and Yang, Lei-Xiang(2008) 'Cucurbit[*n*]urils (*n*=7, 8) binding of camptothecin and the effects on solubility and reactivity of the anticancer drug', Supramolecular Chemistry, 20: 7, 663 — 671
To link to this Article: DOI: 10.1080/10610270701666018
URL: http://dx.doi.org/10.1080/10610270701666018

Supramolecular Chemistry
Vol. 20, No. 7, October–November 2008, 659–665

Taylor & Francis
Taylor & Francis Group

Cucurbit[*n*]urils ($n = 7, 8$) binding of camptothecin and the effects on solubility and reactivity of the anticancer drug

Nan Dong[a,b], Sai-Feng Xue[b]* Qian-Jiang Zhu[b], Zhu Tao[b,c], Yu Zhao[a]* and Lei-Xiang Yang[a]

[a]*Institute of Materia Medical, College of Pharmaceutical Science, Zhejiang University, Hangzhou, P R China;* [b]*Key Laboratory of Macrocyclic and Supramolecular Chemistry of Guizhou Province, Guizhou University, Guiyang, P R China;* [c]*Institute of Applied Chemistry, Guizhou University, Guiyang, P R China*

(*Received 1 July 2007; final version received 4 September 2007*)

The interaction between cucurbit[*n*]uril ($n = 7, 8$)(Q[*n*]) with two forms namely lactone modality and carboxylate modality of anticancer drug camptothecin (CPT) was studied. The results revealed that the combination of Q[*n*] with the lactone form of CPT was observed by electronic absorption spectroscopy, fluorescence spectroscopy and ^{1}H NMR technique in the acid solution (pH 2) and the total stability constants β were also obtained by Job plot with a host:guest ratio of 2:1; while in the phosphate buffer solution (pH 7.4), only Q[8] bound the carboxylate form of CPT in ratio 1:1, but no obvious interaction between Q[7] and the carboxylate form of CPT was observed. The solubility of CPT was enhanced up to about 70 and 8 times at pH 2 due to the formation of interaction complexes with Q[7] and Q[8], respectively, by using phase solubility method. The cytotoxicity tests revealed that compared with the free CPT, the complexes of Q[*n*] and CPT had the same cytotoxic activity on the human lung cancer cell line A549 and murine macrophage cell line P388D1 and the moderate depressed activity on human leukaemia cell line K562.

Keywords: cucurbit[*n*]uril ($n = 7, 8$); camptothecin; interaction; solubility; cytotoxicity

Introduction

Camptothecin (CPT) was first separated from *Camptotheca acuminata* by Wall in 1966 (*1*) and was found to be an effective drug in the treatment of human leukaemia, tummy, liver, lung and bladder cancers. However, its usage was limited due to its appreciable side effects, such as neuro- and nephro-toxicity, nausea, vomiting (*1*) and also its poor solubility in aqueous solution. In order to overcome these limitations, a series of synthetic or semi-synthetic ramification, such as topotecan, irinotecan, 9-AC and 9-NC was produced (*2–4*), and some new drug delivery system, for example, liposome, polymer carrier, microsphere and so on (*5–7*) were developed for the CPT and its analogues.

Cucurbit[*n*]urils (Q[*n*]s) and their derivatives and analogues are a series of barrel-shaped molecules containing a hydrophobic cavity accessible through two identical carbonyl-fringed portals (*8–17*), which are capable of interacting with a variety of organic or inorganic molecules through cavity encapsulation or portal ion–dipole interaction, and the ingression and egression of guests are controlled by the size of the carbonyl portal and cavity. Cucurbit[*n*]uril family has been investigated intensively as a building block for supramolecular assemblies, molecular recognition, separation and so on (*18–25*). In recent years, Q[*n*]s have been explored as drug carriers with the aim of decreasing toxicity, enhancing the solubility, stability and bioavailability of drug molecules (*26–29*).

In this paper, we report a detailed study on the interaction between Q[7] and Q[8] with two forms of CPT: lactone modality and carboxylate modality (referring to Scheme 1), enhancing the solubility of CPT in the presence of Q[*n*] due to the complex formation, and its reactivity of inclusion complex towards human lung cancer cell line A549, human leukaemia cell line K562 and murine macrophage cell line P388D1.

Results and discussion

Interaction between Q[n]($n = 7,8$) *with the lactone form of CPT*

In aqueous solution, there are two forms of CPT which depend on the value of pH (referring to Scheme 1). The lactone form is dominant in the solution of pH < 4.0, while the carboxylate form at pH > 7.2. First, we study the interaction between the lactone form of CPT and Q[*n*] ($n = 7$,8) in 0.01 mol $\cdot$ L^{-1} hydrochloric acid solution (pH 2).

Figure 1(a) shows the variation in the UV spectra obtained with aqueous solutions containing a fixed

*Corresponding authors. Email: sfxue@gzu.edu.cn; dryuzhao@126.com

ISSN 1061-0278 print/ISSN 1029-0478 online

DOI: 10.1080/10610270701666018
http://www.informaworld.com

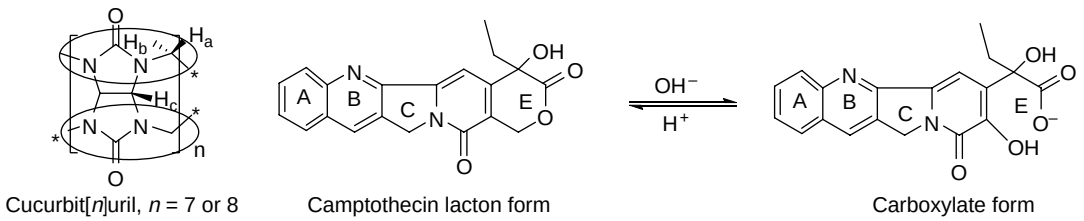

Scheme 1. Structures of Q[7], Q[8] and the two forms of CPT.

concentration of CPT (0.25 μmol) and variable concentrations of Q[7] (0–2.2 μmol). The absorption band of the guest CPT exhibits a progressively lower absorbance at 253 nm, while a progressively higher absorbance at 408 nm as the ratio of $N_{Q[7]}/N_{CPT}$ is increased. A sharp isosbestic point at 375 nm is consistent with a simple interaction between Q[7] and CPT. The absorbance (A) *vs* ratio of moles of the host Q[7] and guest CPT ($N_{Q[7]}/N_{CPT}$) data can be fitted to a 2:1 interaction model for the Q[7]–CPT system at λ_{max} 408 nm (Figure 1(b)). The inset shows the absorbance change (ΔA) *vs* the ratio of $[N_{Q[7]}/(N_{Q[7]} + N_{CPT})]$ data which can also be fitted to a 2:1 interaction model at λ_{max} 408 nm.

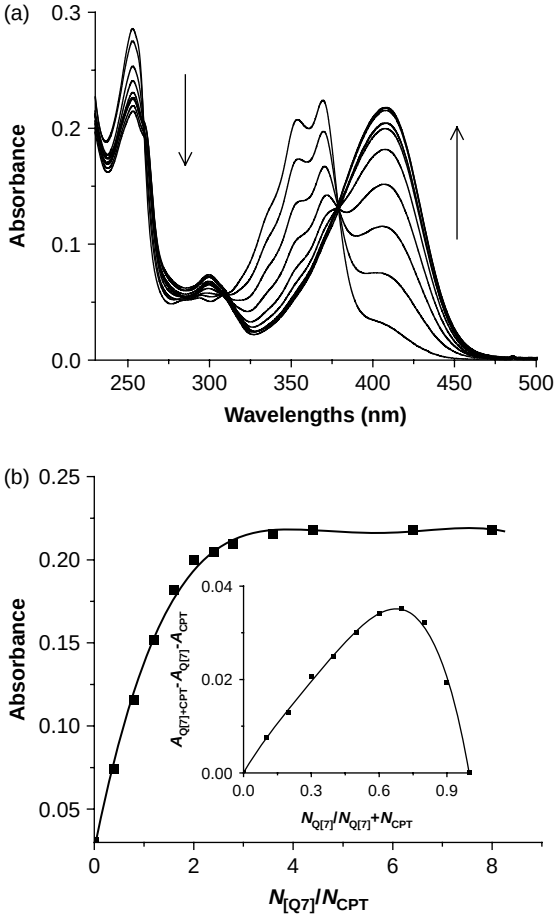

Figure 1. (a) Electronic absorption spectra of CPT (0.25 μmol, 0.01 mol·L^{-1} HCl, pH 2) in the presence of increasing concentrations of Q[7] (0–2.2 μmol) and (b) corresponding absorbance versus $N_{Q[7]}/N_{CPT}$ curve and absorbance (ΔA) *vs* $[N_{Q[7]}/(N_{Q[7]} + N_{CPT})]$ at $\lambda_{max} = 408$ nm (inset).

Figure 2(a) shows the variation in the UV spectra obtained with aqueous solutions containing a fixed concentration of CPT (0.125 μmol) and variable concentrations of Q[8] (0–0.625 μmol). The absorption band of the guest CPT exhibits a progressively lower absorbance at 253 nm. The absorbance (A) *vs* ratio of moles of the host Q[8] and guest CPT ($N_{Q[8]}/N_{CPT}$) data can be also fitted to a 2:1 interaction model for the Q[8]–CPT system at $\lambda_{max} = 253$ nm (Figure 2(b)). The inset shows the absorbance change (ΔA) *vs* the ratio of $[N_{Q[8]}/(N_{Q[8]} + N_{CPT})]$ data which is consistent with the 2:1 interaction model by constructing the corresponding Job plot at $\lambda_{max} = 253$ nm and yields a calculated total stability constants (β) of 3.94×10^{12} L$^2\cdot$ mol^{-2} for the Q[7]–CPT complex and 3.31×10^{12} L$^2\cdot$ mol^{-2} for the Q[8]–CPT complex.

Using fluorescence spectroscopy, similar experiments were performed. The emission spectra of the guest CPT exhibits a progressive increase in fluorescence intensity with a violet shift as the ratio of $N_{Q[7]}/N_{CPT}$ is increased (Figure, see Supplementary information). Both the curves of fluorescence intensity ratio (F/F_0) *vs* $N_{Q[7]}/N_{CPT}$ and ΔI_f *vs* $[N_{Q[7]}/(N_{Q[7]} + N_{CPT})]$ can also be fitted to a 2:1 interaction model for the Q[7]–CPT system at λ_{max} 521 nm. The changes in the spectra was just reverse for the Q[8]–CPT system and the emission spectra of the guest CPT exhibits a simply progressive decrease in fluorescence intensity with a slight red shift as the ratio of $N_{Q[8]}/N_{CPT}$ is increased (Figure, see Supplementary information). Both the curves of fluorescence intensity ratio (F/F_0) *vs* $N_{Q[8]}/N_{CPT}$ and ΔI_f *vs* $[N_{Q[8]}/(N_{Q[8]} + N_{CPT})]$ can also be fitted to a 2:1 interaction model for the Q[8]–CPT system at λ_{max} 433 nm.

The measured data from the Job plots yielded calculated total stable constants (β) 4.31×10^{12} L$^2\cdot$ mol^{-2} and 3.01×10^{12} L$^2\cdot$ mol^{-2} for Q[7]–CPT and Q[8]–CPT complexes, respectively. The values of β are reasonably consistent with average values of 3.94×10^{12} L$^2\cdot$ mol^{-2}

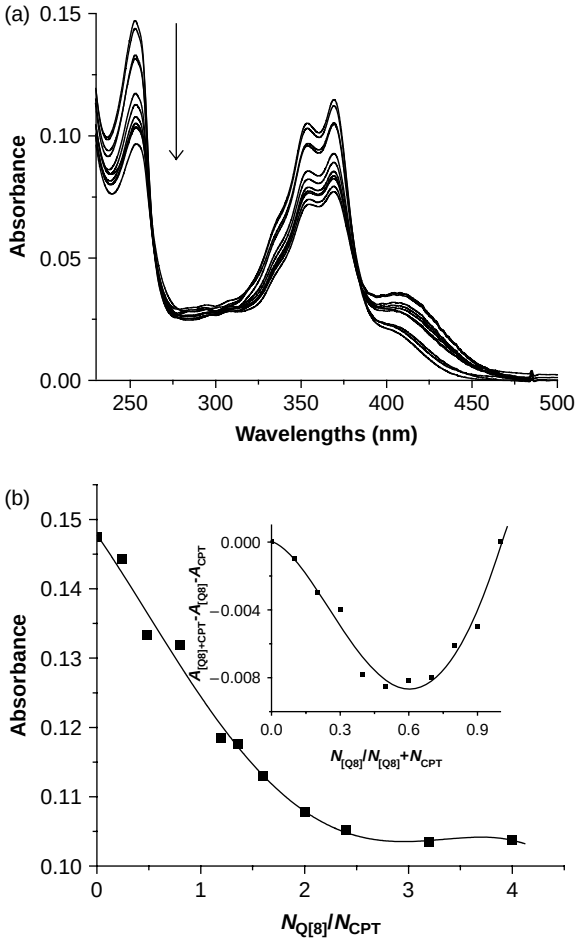

Figure 2. (a) Electronic absorption spectra of CPT (0.125 μmol, 0.01 mol·L^{-1} HCl, pH 2) in the presence of increasing concentrations of Q[8] (0–0.625 μmol) and corresponding absorbance *vs* $N_{Q[8]}/N_{CPT}$ curve (b) and absorbance (ΔA) *vs* $[N_{Q[8]}/(N_{Q[8]}+N_{CPT})]$ at $\lambda_{max} = 253$ nm (inset).

and 3.31×10^{12} L^2·mol^{-2} based on the UV spectroscopy method.

Figure 3 shows the ^{1}H NMR spectra of (a) CPT, (b) complex of Q[7]–CPT and (c) Q[8]–CPT. When compared with the proton resonances of the unbound CPT (*30*, *31*), the signals corresponding to the protons on C_7, C_9, C_{10}, C_{11} and C_{12} of the bound CPT exhibit an upfield shift which is characteristic of this part of the molecule encapsulated in the Q[7] or Q[8] cavity (*32*), while the signals of the protons on C_{14}, C_{18} and C_{19} of the bound CPT experience a downfield shift which is characteristic of the protons of this part of molecule sitting just outside the carbonyl portal of the host Q[7] or Q[8] (*33*). There is a significant downfield shift for the proton on the carbon 14 of the bound CTP in both cases, the proton experienced a downfield shift by 1.20 ppm for the Q[7]–CPT system, while 0.6 ppm for the Q[8]–CPT system. Such a downfield shift of a proton resonance has

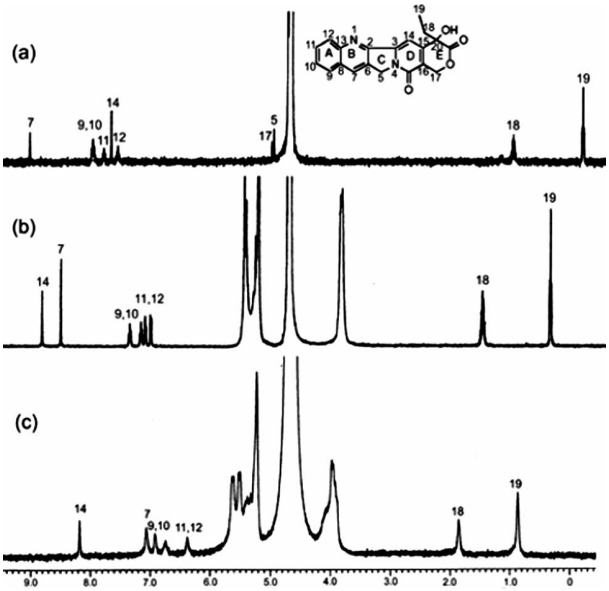

Figure 3. ^{1}H NMR spectra of (a) CPT, (b) inclusion complexes Q[7]–CPT and (c) Q[8]–CPT, respectively, in D_2O.

been observed only in the ^{1}H NMR spectra of Q[n = 6–8]-imidazo[4,5, *f*]1,10-phenanthroline and it derivates systems in which the imidazo moiety of imidazo [4,5, *f*]1,10-phenanthroline threaded through the cavity of the Q[n], and the proton resonances of imidazo and 1,10-phenanthroline moieties experienced a significant downfield shift by about 1.5 ppm (*34*, *35*). On comparing the ^{1}H NMR spectrum of the Q[7]–CPT complex with that of the of Q[8]–CPT complex, one can see that the signal corresponding to the proton on carbon 7 of CPT in Q[8]–CPT exhibits a more significant upfield shift than that in Q[7]–CPT due to the difference in the size of portals and cavity of the host Q[7] and Q[8]. The larger the sizes of portals and cavity are, the deeper the CPT inserts in the cavity of a Q[n] and the more significant is upfield shift the proton exhibits.

The most noticeable effect is the host–guest interaction ratio. A comparison of the integrals of the protons of the bound CPT with the protons of Q[7] or Q[8] revealed the complexes of Q[7]–CPT and Q[8]–CPT to be a 1:1 host:guest species. This behaviour is not consistent with the results from the electronic absorption spectroscopy and fluorescence spectroscopy. Generally, ^{1}H NMR technique is an effective method for detecting host–guest inclusion complex by the shielding or deshielding effects of the protons on the bound guest. However, it is hard to tell the portal interaction between the host and the guest. For the title guest, it has a large size so that the title host cannot encapsulate it entirely. However, it offers a hydrophobic end – the quinoline moiety, which is definitely included in the cavity of a Q[n = 7 or 8], while the hydrophilic end – the carbonyl

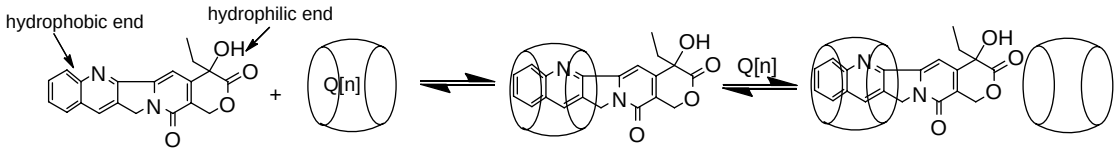

Scheme 2. Possible interaction model between Q[*n*] and CPT.

group and OH group at the E ring of CPT could interact with carbonyl group of another Q[*n*] through hydrogen bond, which is in agreement with the results obtained by electronic absorption spectroscopy and fluorescence spectroscopy. The Scheme 2 shows possible interaction model between Q[*n*] and CPT.

Phase solubility study

The absorbance of a saturated solution of CPT was increased upon increasing the Q[*n*] concentration, which explained the effect of enhancing the solubility to nearly insoluble CPT molecule in the presence of Q[*n*], as shown in Figure 4.

However, the UV–vis study (referring to Figures 1 and 2) revealed that the presence of Q[*n*] could interfere with the spectrophotometry assay of CPT, hence the solubility of CPT in the presence of Q[*n*] in an aqueous solution of pH 2 could be determined in DMSO solution (*36*, *37*) due to no obvious interaction between the host and the CPT, which was further confirmed by ^{1}H NMR (Figure, see Supplementary information).

According to the phase solubility experimental procedure, the phase solubility graphs of CPT in the presence of Q[7] or Q[8] are presented in Figure 5(a) and (b), respectively, which could be classified as Ap-type and An-type, respectively, defined by Higuchi and Connors (*38*) and the bent curves indicated the formation of higher order complexes in solution (*39*, *40*). In the range of low concentration for Q[7]–CPT complex, the phase solubility graph of CPT was linear which means that the 1:1 complex was formed and the apparent stability constant K was calculated by following equation (*41–44*):

$$K = \frac{\text{slope}}{S_0 \times (1 - \text{slope})} \quad (1)$$

where S_0 is the intrinsic solubility of CPT in an aqueous solution of pH 2. Based on Equation (1), $K = 1.64 \times 10^6\,\text{L}\cdot\text{mol}^{-1}$ and $S_0 = 5.95 \times 10^{-6}\,\text{mol}\cdot\text{L}^{-1}$ were achieved.

The effect of enhancing the solubility of Q[*n*] to CPT was displayed in Table 1. The results revealed that the solubility of CPT was increased due to the complex formation between Q[*n*] and CPT.

Interaction between Q[n]($n = 7,8$) *and the carboxylate form of CPT*

Similar experiments have been performed for the carboxylate form of CPT, which is dominating in the phosphate buffer solution (pH 7.4) by using UV–vis, fluorescence spectroscopy and phase solubility method. The results revealed no interaction between Q[7] and CPT under such a basic condition. Although there was no notable change in the intensity of absorbance and fluorescence after addition of Q[8] to the solution of CPT, the solubility of CPT was increased with the

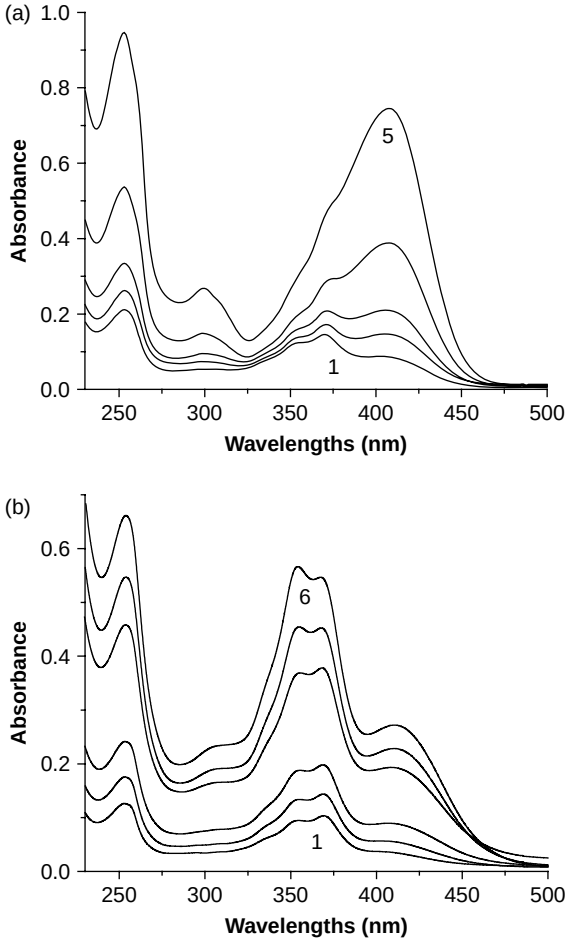

Figure 4. UV–vis spectra of a saturated solution of CPT in the presence of Q[*n*] in 0.01 mol·L^{-1} HCl (pH 2) ((a) $C_{Q[7]}$ 1–5 from 2.6×10^{-5} to 1.2×10^{-4}mol·L^{-1}and (b) $C_{Q[8]}$ 1–6 from 2×10^{-6}–2×10^{-5}mol·L^{-1}).

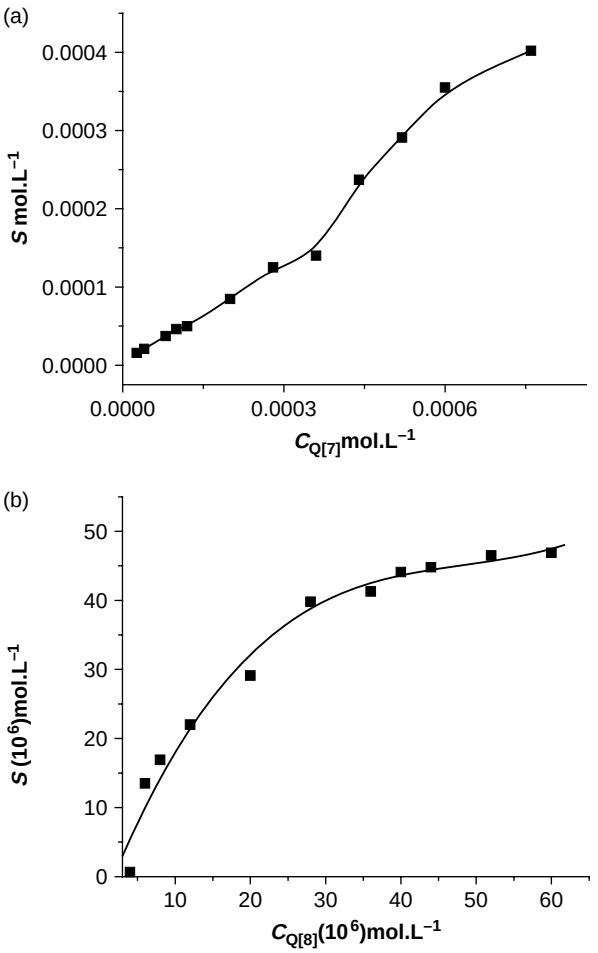

Figure 5. Phase solubility graph of CPT in the presence of (a) Q[7] and (b) Q[8], respectively.

increase in Q[8] concentration (Figures, see Supplementary information). The linear plot of the solubility of CPT indicates the formation of host and guest in a ratio of 1:1. The solubility equation is $S = 9.46 \times 10^{-6} + 0.0896C$ ($r = 0.984$) with $K_{Q[8]-CPT} = 1.01 \times 10^4\,L \cdot mol^{-1}$. This outcome shows that the deprotonation of the N atoms of CPT at a higher pH value (7.4) could depress the interaction of the ion–dipole and hydrogen bonding between Q[*n*] and CPT, while the size of Q[*n*] embodies its importance for the recognition as a host, therefore, the Q[8]–CPT complex with a lower stability constant was observed.

Table 2. Comparison of inhibition (IC_{50} $\mu mol \cdot L^{-1}$) activity for CPT, Q[7]–CPT and Q[8]–CPT.

Cell line	CPT	Q[7]–CPT	Q[8]–CPT	Q[7]	Q[8]
A549	7.76	6.36	6.78	>100	>100
K562	0.43	0.93	1.13	>100	>100
P388D1	2.47	2.38	2.98	>100	>100

In vitro *antitumour activity assay*

To investigate the effect of the encapsulation of the drug on cytotoxicity, a preliminary *in vitro* assay of Q[7]–CPT and Q[8]–CPT was carried out against various cell lines including human non-small cell lung A549, human leukaemia cell line K562 and murine macrophage cell line P388D1. The results revealed that for the A549 and P388D1 cell lines, the inclusion complexes maintained their activity while a moderate decrease in activity was observed for K562 (referring to Table 2). Experimental results also revealed that Q[7] and Q[8] had no cytotoxic effect on these cell lines.

Conclusions

The interactions between cucurbit[*n*]uril ($n = 7, 8$) with the two forms of camptothecin (lactone modality and carboxylate modality) were studied by UV–vis, fluorescence, ^{1}H NMR and phase solubility method. The results revealed that the combination between the Q[*n*] and the lactone form of CPT was observed in the acid solution (pH 2) but only the Q[8]–CPT complex could be formed in the phosphate buffer solution (pH 7.4), which indicates that in addition to van der Waals interaction, size effect and hydrophobic effect, the ion–dipole and hydrogen bonding play an important role in the formation of a stable complex (*45*). It is the combination of host and guest that acts on the effect of enhancing the solubility to insoluble CPT compound, and about 70 and 8 times increase to the solubility of CPT belonging to Q[7] and Q[8], respectively. A preliminary *in vitro* assay revealed that for the A549

Table 1. The effect of enhancing solubility for Q[7] and Q[8].

$C_{Q[7]}$ ($10^5 mol \cdot L^{-1}$)	0	2.6	8.0	20	36	52	76
S ($10^5 mol \cdot L^{-1}$)	0.595	1.57	3.72	8.47	14.3	29.1	40.2
S/S_0		2.64	6.25	14.2	23.5	48.9	67.7
$C_{Q[8]}$ ($10^6 mol \cdot L^{-1}$)	0	2.0	8.0	20	36	52	60
S ($10^6 mol \cdot L^{-1}$)	5.95	6.46	16.9	29.1	41.3	46.5	46.9
S/S_0		1.08	2.84	4.89	6.94	7.82	7.88

*S/S_0 (factor of enhancing solubility).

and P388D1 cell lines, Q[7]–CPT and Q[8]–CPT complexes maintained CPT activity while a moderate decrease in the activity was observed for K562.

Experimental

Materials

Q[7] and Q[8] were prepared at the Applied Chemistry Institute, Guizhou University, according to literature (*46*). CPT was purchased from JiangYuan Nature Product Company (purity > 98.32%, Si Chuan, China); its hydrochloric salt form was prepared for the advantage of the NMR monitor. A $2.874 \times 10^{-4}\,mol \cdot L^{-1}$ stock solution of CPT was prepared with methanol. DMSO and methanol are analytical reagents. Scheme 1 shows the structures of CPT and Q[*n*].

UV–vis spectroscopy and fluorescence spectroscopy

All absorption and fluorescence measurements except Job method were performed on solutions that contained different concentrations of Q[*n*] with a fixed concentration of guest CPT in 1 cm^2 quartz cuvettes. Absorption spectra were measured on an Agilent PH8453 UV–vis spectrophotometer, while fluorescence spectra were measured on a Cary Eclisper spectrometer with excitation and emission band width of 5 nm.

^{1}H NMR spectroscopy

^{1}H NMR spectra were obtained using a Varian 400 instrument in D_2O or in DMSO-d_6, and were referenced in ppm with respect to a TMS standard.

Phase solubility method

The linear range was calibrated using 10 different concentrations of CPT (in DMSO) solution (5.75×10^{-6}–$1.15 \times 10^{-4}\,mol \cdot L^{-1}$) to establish the calibration curve of CPT spectrophotometrically at $\lambda_{368\,nm}$.

A series of mixtures with excessive CPT and variable concentrations of Q[*n*] were put in 0.01 M HCl by vibrating for 1 h on an ultrasonic equipment. The suspension was stirred at room temperature in a dark room until equilibrium was reached (1 week). The saturated solutions with the Q[*n*]–CPT complex were passed through a membrane filter (0.45 μm) to remove the insoluble residue. The solvent ($0.01\,mol \cdot L^{-1}$ HCl) of a 1 mL filtrate was removed on a rotary evaporator, and dissolved in 10 mL measuring flask with DMSO. Thus, the amount of CPT in the Q[*n*]–CPT complexes was obtained spectrophotometrically at $\lambda_{368\,nm}$ by comparing with the calibration curve of CPT, and the phase solubility diagram was constructed by plotting the total dissolved CPT concentration against the total Q[*n*] concentration in 0.01 M HCl.

Phase solubility diagram of CPT in the phosphate buffer solution (pH 7.4) with Q[*n*] can be obtained by using a similar method.

Preparation of inclusion complexes Q[7]–CPT and Q[8]–CPT

The binary systems of CPT–Q[*n*] were prepared by co-evaporation. Q[*n*]($n = 7, 8$) and CPT in a molar ratio of 2:1 were added to 25 mL of $0.01\,mol \cdot L^{-1}$ HCl solution and stirred for 24 h at 45°C. The hot solution was filtered using a 0.45 μm membrane filter and dried to obtain a powder. The powder was washed three times with acetone and the solvent eliminated by vacuum evaporation at 45°C.

In vitro *antitumour activity assay*

An *in vitro* antitumour activity assay of CPT, Q[7]–CPT, Q[8]–CPT, Q[7] and Q[8] was performed by a MTT method at the Institute of Materia Medical of Zhejiang University.

Acknowledgements

This work was supported by the Natural Science Foundation of China (Grant No. 20662003), 'Chun-Hui' Fund of Chinese Ministry of Education, International Collaborative Project of Guizhou Province and Governor Foundation of Guizhou Province (Grant No. 2007400108).

References

(1) Wal, M.E.; Wani, M.C.; Cook, C.E. *J. Am. Chem. Soc.* **1966**, *88*, 3888–3890.
(2) Whitacre, C.M.; Zborowska, E.; Willson, J.K. *Clin. Cancer Res.* **1999**, *5*, 665–672.
(3) Fletcher, T.M.; Sun, D.; Salazar, M. *Biochemistry* **1998**, *37*, 5536–5541.
(4) Panayotis, P.; Zhiyong, H.; Devasis, C. *Drug. Future* **1999**, *24*, 1311–1323.
(5) Daoud, S.S.; Fetouh, M.I.; Giovaneua, B.C. *Anti-cancer Drug* **1995**, *6*, 83–93.
(6) Greenwald, R.B.; Pendri, A.; Conover, C.D. *J.Med. Chem.* **1996**, *39*, 1938–1940.
(7) Mallery, S.R.; Shenderova, A.; Pei, P. *Anticancer Res.* **2001**, *21*, 1713–1722.
(8) Freeman, W.A.; Mock, W.L.; Shih, N.Y. *J. Am. Chem. Soc.* **1981**, *103*, 7367–7368.
(9) Day, A.I.; Arnold, A.P. WO 0068232, 2000, 8.
(10) Kim, J.; Jung, I.S.; Kim, S.Y.; Lee, E.; Kang, J.K.; Sakamoto, S.; Yamaguchi, K.; Kim, K. *J. Am. Chem. Soc.* **2000**, *122*, 540–541.
(11) Day, A.I.; Blanck, R.J.; Arnold, A.P.; Lorenzo, S.; Lewis, G.R.; Dance, I. *Angew. Chem. Int. Ed.* **2002**, *41*, 275–277.

(12) Zhao, J.; Kim, H.J.; Oh, J.; Kim, S.Y.; Lee, J.; Sakamoto, W.S.; Yamaguchi, K.; Kim, K. *Angew. Chem. Int. Ed.* **2001**, *40*, 4233–4235.
(13) Sasmal, S.; Sinha, M.K.; Keinan, E. *Org. Lett.* **2004**, *6*, 1225–1228.
(14) Jon, S.Y.; Selvapalam, N.; Oh, D.H.; Kang, J.K.; Kim, S.Y.; Jeon, Y.J.; Lee, J.W.; Kim, K. *J. Am. Chem. Soc.* **2003**, *125*, 10186–10187.
(15) Isobe, H.; Sato, S.; Nakamura, E. *Org. Lett.* **2002**, *4*, 1287–1289.
(16) Day, A.I.; Arnold, A.P.; Blanch, R.J. *Molecules* **2003**, *8*, 74–84.
(17) Zhao, Y.J.; Xue, S.F.; Zhu, Q.J.; Tao, Z.; Zhang, J.X.; Wei, Z.B.; Long, L.S.; Hu, M.L.; Xiao, H.P.; Day, A.I. *Chin. Sci. Bull.* **2004**, *49*, 1111–1117.
(18) Lagona, J.; Fettinger, J.C.; Isaacs, L. *Org. Lett.* **2003**, *5*, 3745–3747.
(19) Lagona, J.; Mukhopadhyay, P.; Chakrabarti, S.; Isaacs, L. *Angew. Chem. Int. Ed.* **2005**, *44*, 4844–4870.
(20) Lee, J.W.; Samal, S.; Selvapalam, N.; Kim, H.J.; Kim, K. *Acc. Chem. Res.* **2003**, *36*, 621–630.
(21) Gerasko, O.A.; Samsonenko, D.G.; Fedin, V.P. *Russ. Chem. Rev.* **2002**, *71*, 741–760.
(22) Elemans, J.A.A.W.; Rowan, A.E.; Nolte, R.J. M. *Ind. Eng. Chem. Res.* **2000**, *39*, 3419–3428.
(23) Hubin, T.J.; Kolchinski, A.G.; Vance, A.L.; Busch, D.H. *Adv. Supramol. Chem.* **1999**, *5*, 237–357.
(24) Mock, W.L. *Top. Curr. Chem.* **1995**, *175*, 1–24.
(25) Cintas, P. *J. Incl. Phenom. Molec. Reco. Chem.* **1994**, *17*, 205–220.
(26) Wheate, N.J. *Aust. J. Chem.* **2006**, *59*, 354.
(27) Jeon, Y.J.; Kim, S.Y.; Ko, Y.H.; Sakamoto, S.; Yamagchi, K.; Kim, K. *Org. Biomol. Chem.* **2005**, *3*, 2122–2125.
(28) Wheate, N.J.; Day, A.I.; Blanch, R.J.; Arnold, A.P.; Cullinance, C.; Collins, J.G. *Chem. Commun.* **2004**, 1424–1425.
(29) Buschmann, H.-J.; Cleve, E.; Jansen, K.; Schollmeyer, E. *Anal. Chim. Acta.* **2001**, *437*, 157–163.
(30) Kingsburg, W.D.; Boehm, J.C.; Jakas, D.R. *Med. Chem.* **1991**, *34*, 98–107.
(31) Xu, C.-Y.; Huang, M.-Z.; Xue, C.-X. *Spectrosc. Spect. Anal.* **2004**, *24*, 573.
(32) Wagner, D.; Stojanovic, N.; Day, A.I.; Blanch, R.J. *J. Phys. Chem. B* **2003**, *107*, 10741–10746.
(33) Saleh, N.; Al-Rawashdeh, N.A. F. *J. Fluoresc.* **2006**, *16*, 487–493.
(34) Wang, Q.-L.; Xue, S.-F.; Mu, L.; Zhu, Q.-J.; Tao, Z.; Zhang, J.-X. *Spectrosc. Spect. Anal.* **2006**, *26*, 499–504.
(35) Xiang, S.-C.; Tao, Z.; Hu, Y.; Xiang, Z.-M.; Xue, S.-F.; Zhu, Q.-J.; Zhang, J.-X. *Chin. J. Org. Chem.* **2005**, *25*, 1208–1214.
(36) Feng, G.-Z.; Lu, K.; Li, H.-P. *Spectrosc. Spect. Anal.* **2004**, *24*, 1099.
(37) Wang, H.; Fang, Y.; Mei, M.-H. *Acta Phys.-Chim. Sinica* **2002**, *21*, 603.
(38) Higuchi, T.; Connors, K.A. *Adv. Anal. Chem. Instrum.* **1965**, *4*, 117–210.
(39) Szejeli, J.; Hungary, C.B. *Compr. Supermol. Chem.* **1996**, *3*, 196.
(40) Shen, Y.-L.; Ying, W.; Yang, S.-H.; Wu, L.-M. *Spectrochim. Acta A* **2006**, *65*, 169–172.
(41) Liu, L.-X.; Zhu, S.-Y. *Carbohyd. Polym.* **2007**, *68*, 472–476.
(42) Li, N.; Xiong, Y.-H.; Li, Z.-G.; Jin, X.-H.; Wu, Y.-N. *J. Pharmaceut. Biomed.* **2005**, *38*, 370–374.
(43) Crupi, V.; Ficarra, R.; Guardo, M.; Majolino, D.; Stancanelli, R.; Venuti, V. *J. Pharmaceut. Biomed.* **2007**, *44*, 110–117.
(44) Figueiras, A.; Sarraguca, J.M. G.; Carvalho, R.A.; Pais, A.A. C. C.; Veiga, F.J. B. *Pharmaceut. Res.* **2007**, *24*, 377–389.
(45) Buschmann, H.-J.; Schollmeyer, E.; Mutihac, L. *Thermochim. Acta.* **2003**, *399*, 203–208.
(46) Buschmann, H.-J.; Cleve, E.; Jansen, K.; Wego, A.; Schollmeyer, E. *Mat. Sci. Eng. C* **2001**, *14*, 35–39.